THE JOURNAL OF PHYSICAL CHEMISTRY B

Article

pubs.acs.org/JPCB

Solid-State NMR/Dynamic Nuclear Polarization of Polypeptides in Planar Supported Lipid Bilayers

Evgeniy S. Salnikov,[†] Hiba Sarrouj,[†,‡] Christian Reiter,[‡] Christopher Aisenbrey,[†] Armin Purea,[‡] Fabien Aussenac,[§] Olivier Ouari,[∥] Paul Tordo,[∥] Illya Fedotenko,[∥] Frank Engelke,*[,‡] and Burkhard Bechinger*[,†]

[†]Institute of Chemistry, University of Strasbourg/CNRS, UMR7177, 67070 Strasbourg, France

[‡]Bruker BioSpin, Silberstreifen, 76287 Rheinstetten, Germany

[§]Bruker BioSpin, 34, rue de l'Industrie, 67166 Wissembourg, France

[∥]Aix Marseille Université, CNRS, Institut de Chimie Radicalaire, UMR 7273, 13013 Marseille, France

Supporting Information

ABSTRACT: Dynamic nuclear polarization has been developed to overcome the limitations of the inherently low signal intensity of NMR spectroscopy. This technique promises to be particularly useful for solid-state NMR spectroscopy where the signals are broadened over a larger frequency range and most investigations rely on recording low gamma nuclei. To extend the range of possible investigations, a triple-resonance flat-coil solid-state NMR probe is presented with microwave irradiation capacities allowing the investigation of static samples at temperatures of 100 K, including supported lipid bilayers. The probe performance allows for two-dimensional separated local field experiments with high-power Lee−Goldberg decoupling and cross-polarization under simultaneous irradiation from a gyrotron microwave generator. Efficient cooling of the sample turned out to be essential for best enhancements and line shape and necessitated the development of a dedicated cooling chamber. Furthermore, a new membrane-anchored biradical is presented, and the geometry of supported membranes was optimized not only for good membrane alignment, handling, stability, and filling factor of the coil but also for heat and microwave dissipation. Enhancement factors of 17-fold were obtained, and a two-dimensional PISEMA spectrum of a transmembrane helical peptide was obtained in less than 2 h.

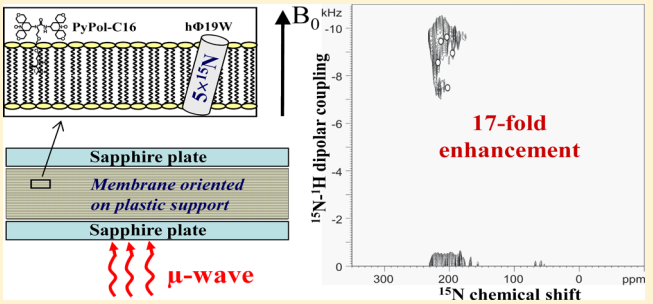

Solid-state NMR spectroscopy is a powerful method for the structural investigation of membrane polypeptides and has provided valuable information about the conformation, topology, and dynamics in lipid bilayer environments. Two fundamentally different approaches have been developed for the structural investigation of biological macromolecules, namely, magic angle sample spinning (MAS) and oriented solid-state NMR, which both have been used to determine important structural and dynamic features from uniformly or selectively labeled membrane proteins.[1−8]

The latter approach consists in orienting membranes with respect to the magnetic field direction and exploiting the large anisotropies of the chemical shifts, dipolar and quadrupolar couplings that are obtained from such aligned samples.[9] This technique has been successful in the structural analysis of, for example, the transmembrane peptides gramicidin A, Vpu, alamethicin, and phospholamban (e.g., see refs 2,10) but has also been applied to other, larger and functionally more complex membrane proteins (e.g., see ref 8). Oriented solid-state NMR has also been used to monitor structural changes, for example, of phospholamban when bound to the large SERCA protein.[2] Whereas for some polypeptides, accurate structures have been determined,[2,10,11] this approach also provides detailed information about the tilt and rotational pitch angles of membrane-inserted helices where it can follow even small changes (e.g., of 1°) in structure or topology.[12,13] Combining distance constraints and angular constraints from oriented solid-state NMR has resulted in a refined structural analysis.[1,2,8,11]

A major problem of these approaches remains the inherently low signal intensity of NMR spectroscopy, which results in the necessity to investigate relatively large quantities of polypeptides. The problem is already apparent in solution-state NMR but pronounced in solid-state NMR spectroscopy where the line width is larger and concomitantly the signal-to-noise reduced (assuming the same signal integral). In particular, in oriented samples in many cases, the peptides as a whole or individual sites of a protein in phospholipid bilayers can exhibit an inherent and functionally important distribution of conformations and alignments which cause broad but highly

Received: July 29, 2015
Revised: October 20, 2015

ACS Publications © XXXX American Chemical Society

DOI: 10.1021/acs.jpcb.5b07341
J. Phys. Chem. B XXXX, XXX, XXX−XXX

informative line shapes,[14,15] albeit other examples exist where much sharper signal intensities are observed.[2,10,11]

In this context, dynamic nuclear polarization (DNP) techniques have been developed over the last decades[16,17] and made commercially available recently.[18] By transferring the large polarization of unpaired electrons via the irradiation of an EPR transition, a large signal-to-noise enhancement of the ^{1}H NMR signal can be achieved, with a theoretical maximum of 660 (γ_e/γ_n). Although most studies using DNP in solid-state NMR experiments have been performed so far on samples rotating at the magic angle, the signal enhancements by DNP should be even more valuable for oriented membrane samples where the broad inherent line shapes make it more difficult to obtain reasonable signal-to-noise ratios and where additional experimental restraints result from the need to align the samples. Good sample alignment often requires dilution of the polypeptide in a lipid matrix (typically 1/50 to 1/200 mol/mol). Furthermore, much of the coil volume is occupied by the solid supports onto which the membranes are oriented[19−21] or by aqueous solution in order to comply with the particular conditions required to align bicellar systems.[22,23]

However, it should be taken into consideration that DNP/solid-state NMR experiments are performed under very particular conditions, namely, the possibility to irradiate the sample with microwaves of several Watts matching the EPR transitions at high magnetic fields (263 GHz for a 9.4 T NMR magnet) and the need to slow down the relaxation rates of the unpaired electrons by keeping the sample at low temperatures.[17,18,24] Therefore, the best signal enhancements are obtained when the samples are cooled with liquid helium[24] or liquid nitrogen.[17,18] It remains possible to perform DNP/solid-state NMR experiments also at increased, even ambient temperatures, but in these cases more modest enhancements are observed.[25,26] In prior work, we have therefore performed some proof-of-concepts studies to test if the technology can be applied to oriented membranes.[27,28] With only MAS probes available at the time, a lipid bilayer carrying a transmembrane model peptide labeled with ^{15}N at one site was oriented on a polymer sheet, wrapped into a cylinder, and investigated under low (around 1 kHz) and fast (8 kHz) MAS spinning conditions. The resulting ^{15}N sideband intensities are indicative that the membranes remain oriented at 100 K, and under such MAS conditions, up to 17-fold signal enhancements have been obtained when mixing bTbK or TOTAPOL biradicals into the oriented membranes.[27,28]

Because only a low-temperature MAS probe for DNP/solid-state NMR was made available with the commercial systems,[18] converting this probe for static measurements following previous flat-coil NMR probe developments[29] seems on first view straightforward. However, the geometries of oriented membrane samples result in a number of additional considerations.

First of all, for the current three-spin model of cross-effect DNP, the effect of MAS has been shown to be important in promoting the required mixing of direct product spin states.[31] Sample spinning thereby helps in increasing the efficient DNP signal enhancements by the cross effect in frozen samples carrying biradicals.[30−32] As a consequence, a larger fraction of the spins become polarized under MAS, and the signal enhancements obtained from static samples are several-fold decreased when compared to samples undergoing MAS in the optimal frequency range[18,32] even if some MAS-induced spin depolarization has been described to reduce the overall gain.

Second, the cooling gas arrives at the sample from one side and flows around the MAS rotor. At the same time, the sample rotates quickly with the sample being close to the rotor walls. This helps in cooling the sample evenly. Notably, the better enhancements observed with sapphire when compared to zirconia rotors were associated with the better thermal conductivity of the latter illustrating the importance of homogeneous cooling efficiency,[33] albeit the influence of the dielectric constant of the material and its wall thickness are also important and currently under investigation. In contrast, additional precautions have to be taken to ensure a homogeneous and efficient cooling of the static oriented samples, which tend to also be relatively voluminous where the length exceeds the width and both are larger than their height.

Third, to be efficient, the microwaves have to penetrate as much of the sample as possible. Once they leave the corrugated waveguide, they have to pass the NMR coil to penetrate the sample. Importantly it has been shown that MAS rotors of appropriate thickness or the presence of dielectric particles in the sample helps the penetration of the microwaves, thereby assuring a more efficient sample irradiation.[34,35] In contrast, the oriented samples are usually only enveloped by plastic and Teflon wrapping and in addition contain stacks of solid support and lipid bilayers with a repetition distance (typically 20−30 solid supports for a 3 mm stack) close to the wavelength of the microwaves (10^{-3} m). The effects of such an arrangement on the microwave penetration have so far not been investigated, and tests of different sample geometries will be reported here.

MATERIALS AND METHODS

The phospholipid 1-palmitoyl-2-oleoyl-*sn*-glycero-3-phosphocholine (C16:0, C18:1-PC, POPC) is from Avanti Polar Lipids (Alabaster, AL). $^{15}NH_4Cl$ (99,5% ^{15}N) was purchased from Cambridge Isotope Laboratories (Andover, MA). All commercial material was used without further purification.

Peptide Sequence and Label Positions. The hydrophobic peptide [$^{15}N_5$]- hΦ19W (KKKALLALLALAWALALLALLAKKK) was prepared by solid phase peptide synthesis as described previously.[12] At five subsequent positions, leucine and alanine labeled with ^{15}N were incorporated into the peptide (underlined in the above sequence). The AMUPol and PyPol biradicals were prepared as described previously.[36] The preparation and comparative evaluation of PyPol-C16, a derivative of PyPol bearing a palmitoyl chain, will be described in a separate paper discussing the effect of the polarizing agent structure on the signal enhancement in oriented experiments (Figure S1). The HRMS (ESI) analysis of the compound indicates an m/z of 906.6533 which compares well with the theoretical value of 906.6526 for $C_{49}H_{87}N_5O_{10}$ $[M + H]^+$

Water/Glycerol Sample for DNP. A homogeneous mixture of 1.5 M $^{15}NH_4Cl$ and 10 mM AMUPol dissolved in D_2O/H_2O/glycerol-d_8 30/10/60 by weight was placed in sapphire rotor and used as reference. The temperature dependence of the ^{15}N line width allows for temperature calibration (see Figure S2).

Membrane Samples for DNP. A homogeneous mixture of lipid, peptide, and radical was obtained by codissolving the membrane components in trifluoroethanol. To prepare oriented-POPC membranes, the solution was spread onto ultrathin cover glasses (3 × 8 mm for the DNP probe; 8 × 22 mm for conventional oriented solid-state NMR measurements; thickness 00; Marienfeld, Lauda-Konigshofen, Germany) or High-Density PolyEthylene (HDPE) film (3 × 8 mm,

DOI: 10.1021/acs.jpcb.5b07341
J. Phys. Chem. B XXXX, XXX, XXX−XXX

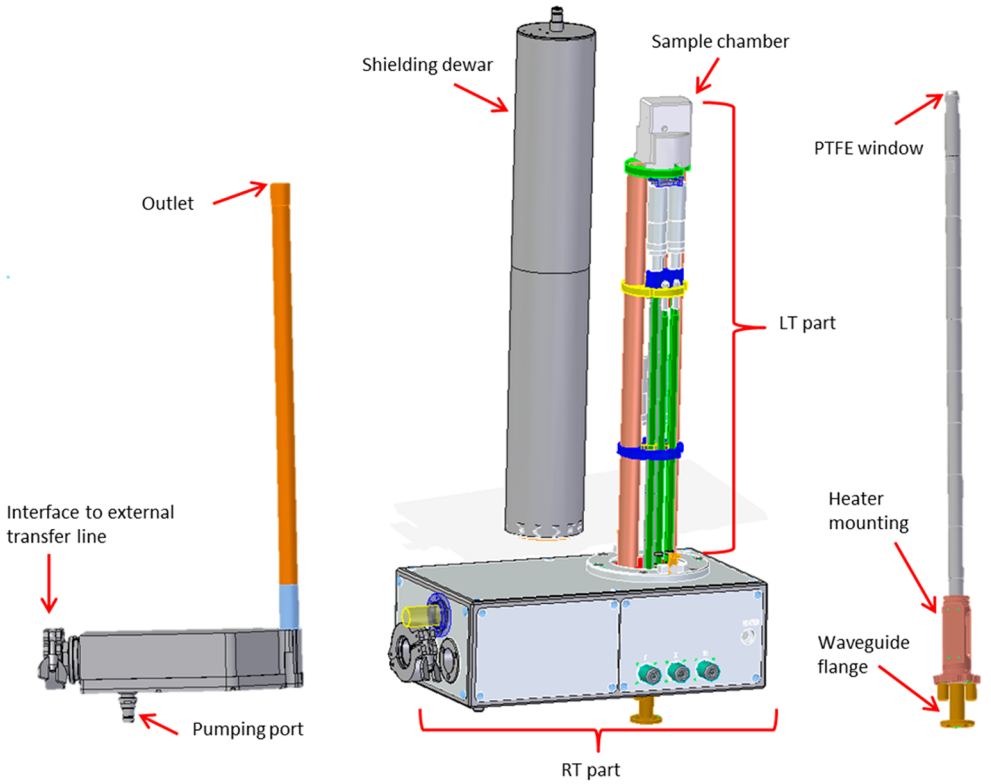

Figure 1. Left side: gas transfer line with ports; center: complete probe with shielding Dewar; right side: waveguide.

Goodfellow, Cambridge, U.K.), dried first in air and followed by high vacuum overnight.[27,37] Thereafter, the sample was equilibrated during a day in an atmosphere of 93% relative humidity of D_2O/H_2O (90/10 by volume). The glass plates were then stacked on top of each other and wrapped in Teflon. The HDPE film with a sample was carefully folded to fit in the coil and flattened in between two sapphire plates of 3 × 8 mm and 0.5−0.8 mm thickness. In the case of nonoriented samples, the POPC suspension was transferred into the 3.2 mm sapphire rotor without mechanical support. The use of partially deuterated "solvent" (lipid, water, and glycerol) channels spin diffusion toward the protonated peptide chain.

DNP/Solid-State NMR. DNP/solid-state NMR measurements were performed using a Bruker BioSpin wide-bore 9.4 T magnet and an Avance III solid-state NMR spectrometer equipped with a gyrotron producing 263 GHz irradiation, a microwave transmission line delivering about 5 W of microwave power at the sample (MAS probe), a cooling unit using liquid nitrogen, and a low-temperature triple resonance 3.2 mm MAS probe.[18] The spectra shown in Figure 3 were obtained using a commercial $^{1}H-^{13}C-^{15}N$ triple resonance MAS probe and setup for low temperatures of ≥100 K (Bruker, Wissembourg, France). An adiabatic CP pulse sequence[38] was used with a spectral width of 29.8 kHz and acquisition, cross-polarization contact, and recycle delay times of 8.6 ms, 0.3 ms, and 3 s, respectively. The ^{1}H $\pi/2$ pulse and spinal64 heteronuclear decoupling field strengths B_1 corresponded to a nutation frequency of 50 kHz. To equilibrate the system before acquisition the sample was exposed to 16 dummy scans. An exponential line-broadening of 100 Hz was applied before Fourier transformation for membrane samples and no line-broadening in the case of water/glycerol. Spectra were externally referenced to $^{15}NH_4Cl$ powder at 40 ppm at room temperature.[39] The DNP signal enhancement was determined as a ratio in the integral signal intensity of MW ON versus MW OFF spectra obtained with identical parameters.

The oriented samples were investigated with a purposely built static solid-state NMR/DNP probe introduced in this paper. The PISEMA spectrum was recorded on 3.3 mg $[^{15}N_5]$-hΦ19W at a nominal temperature of 100 K (where the actual sample temperature depends on the MW irradiation (∼180 K)). The peptide was reconstituted in a POPC membrane at a molar peptide-to-phospholipid ratio of 1/20 and oriented onto a HDPE film. The PyPol-C16 was added in the quantity of 0.2 mg per 20 mg of POPC membrane. A step-by-step protocol for setting up and analyzing the experiment are given in ref 19,40. The effective B_1 field strength during the SEMA pulse train was 50 kHz. During the spin exchange period, the amplitude of the ^{1}H B_1 field was decreased to 40.9 kHz to maintain the Hartmann−Hahn match condition with an effective field along the magic angle of 50 kHz.

RESULTS AND DISCUSSION

Probe Design for Static DNP/Solid-State NMR. The probe used for the static DNP measurements is based on a Cryo-MAS probe equipped with a Dewar style shielding tube, vacuum jacked gas transfer line for sample cooling, and a corrugated waveguide for microwave irradiation (Figure 1). The sample chamber and NMR coil are designed according to the requirements of the sample[29] and the conditions of the combined DNP and NMR experiments, namely, reasonable cross-polarization (CP) performance, proper cooling, and microwave transparency.[34,35]

The radiofrequency (RF) part of the probe consists of two channels connected to a free-standing NMR coil with a 4 × 4 mm cross section and 10 mm length. In order to improve the microwave propagation through the RF coil, the 8.5 turns were

DOI: 10.1021/acs.jpcb.5b07341
J. Phys. Chem. B XXXX, XXX, XXX−XXX

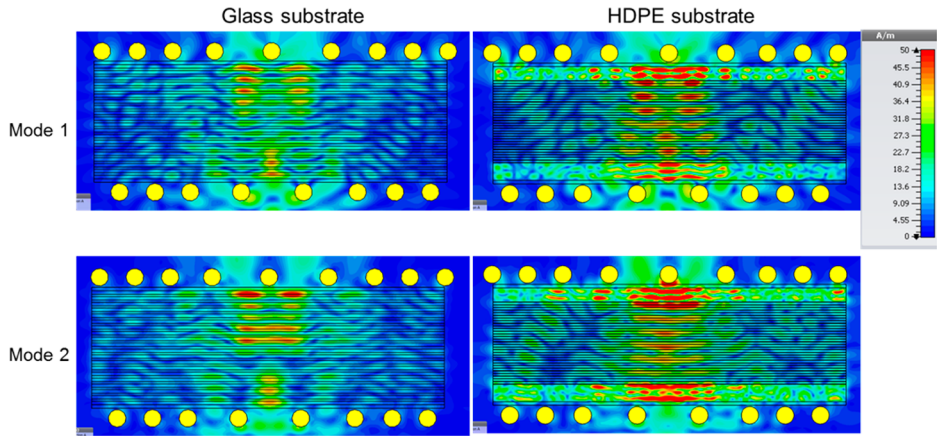

Figure 2. Central cut views through the sample stack showing the absolute H-field distribution.

wound with a variable pitch. The inter turn distance is 1.3 mm at the center and decreases symmetrically toward the coil endings.

As shown in Figure S3, the ^{1}H channel has a capacitive matching coupled to a tuning trimmer that is connected to the NMR coil via a transmission line. To isolate the ^{1}H frequency circuit from the Y-channel tuned to ^{15}N an LC-stop circuit is used. The Y-channel exhibits inductive matching and a tuning trimmer with ports for a shunt capacitor that enables the user to set the tuning range to the desired frequency band. The Y channel frequency is decoupled from the proton channel via grounding at the $\lambda/4$ point of the transmission line. The whole circuit as well as some representative sensitivity values and tuning ranges are illustrated in Figure S3. All trimmers used for this probe have polytetrafluoreethylene (PTFE) dielectric and can be operated at cryogenic temperatures. A third channel (not shown in Figure 1) for ^{13}C or ^{31}P has also been built into the circuit for future use.

In order to enable operation of the probe at temperatures close to 100 K, the probe is separated into two sections (see details in Figure 1). The probe base with all the connectors and interfaces is held at room temperature or close to room temperature by heating foils at several positions. Two of them are there to keep warm the lower part of the microwave guide and another two are in contact with the walls of the probe base. In addition, the probe base is flushed with dry nitrogen gas to keep it free of moisture and to avoid ice forming at the various feed-throughs leading into the cold part of the probe. The flushing gas also helps to distribute the heat and hence to smooth the temperature profile across the surface. For insulating the two probe sections a Vespel capsule with a thickness of approximately 30 mm is used with gastight feed-throughs for all mechanical actuators and RF-lines.

The sample chamber (Figure S4) is made of PTFE and surrounds the NMR coil with the sample. Two Teflon hoses are connected to the chamber guiding the cold gas from the transfer line outlet to the sample. In order to change the sample, the chamber has to be disassembled.

The low-temperature region of the probe is insulated from the magnet shim system by a double-wall evacuated shielding Dewar (Figure 1 center). The sample chamber and all electronics are located inside this section. The cold gas is guided toward the sample chamber via three gas conducting channels inside a vacuum-insulated transfer line, the latter also enabling temperature regulation by means of channel heaters and PT100 temperature sensors. Two of the gas flows enter the sample chamber pointing onto the NMR-coil directly while the third one flushes the outer surface of the chamber. All three flows combine underneath the sample chamber and cool the RF electronics for increased sensitivity. Finally the gas flow leaves the probe through an exhaust pipe. Two thermocouples are used to read the temperature within the sample chamber and in the exhaust pipe, respectively. The heat exchanger used to supply the cold nitrogen gas is a commercially available Bruker LT-MAS cooling cabinet.

Numerical Analysis. Electromagnetic simulations at 263 GHz were carried out using CST Microwave Studio 2014 (CST AG, Darmstadt, Germany) to study the field distribution in the sample. A geometrical model of the waveguide end, coil block, RF coil, and sample stack was generated. Three sample geometries were studied: a sapphire rotor filled with a water/glycerol DNP sample serving as recreation of the reference sample and two biomembrane stacks (one with glass as substrate and one with HDPE).

The glass stack consists of 20 glass layers of 0.1 mm thickness. Between each glass layer, a membrane layer of 0.065 mm width is inserted. Another layer of 0.1 mm PTFE is added on the top and on the bottom of the stack.

The HDPE stack consists of 32 layers of 0.01 mm HDPE and 31 layers of membrane sample, again with a thickness of 0.065 mm. On the bottom, a Sapphire layer of 0.5 mm is added, and another one of 0.4 mm on the top. As in the case of the glass stack, a PTFE layer of 0.1 mm is added on top and bottom. The overall dimensions of both stacks are 10 mm × 2.4 mm × 3.435 mm.

Dielectric parameters of the various materials are set according to published data.[34,35,41] For the bilayer sample, the dielectric parameters are taken from paraffin since a large part of the sample consists of lipids. A hexagonal mesh is used for spatial discretization. One or more cells are present in the direction of stacking to ensure that all material changes are adequately resolved. The cell dimensions are typically between 10 and 80 μm.

At the side of the waveguide opposing the coil, a waveguide port is placed and excited with an HE11 mode. The polarization angle can be set such that the E-field of the mode is either perpendicular (mode 1) or parallel (mode 2) to the coil windings. The simulations are carried out using the time-domain solver, and three-dimensional field data for the E and H fields is obtained. Cut views of the absolute H field

DOI: 10.1021/acs.jpcb.5b07341
J. Phys. Chem. B XXXX, XXX, XXX−XXX

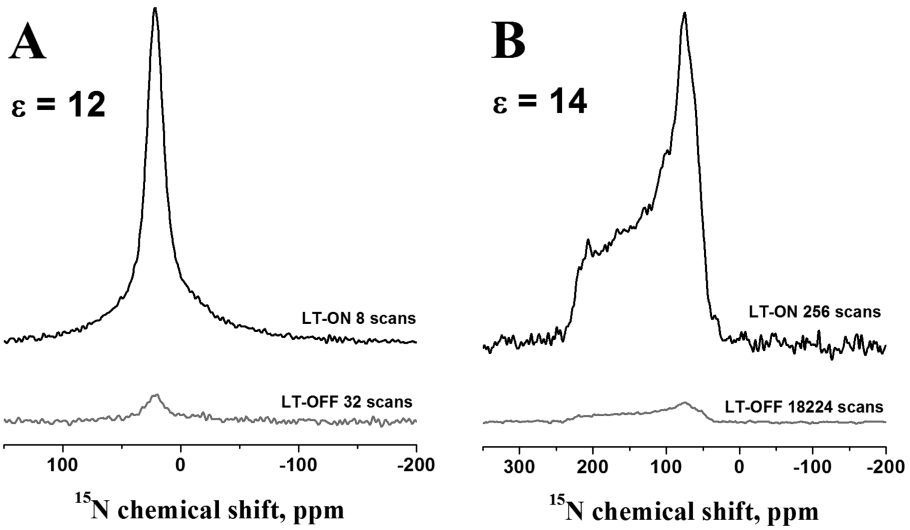

Figure 3. Proton-decoupled ^{15}N solid-state NMR spectra of 1.5 M $^{15}NH_4Cl$ in glycerol/water ("DNP juice")/AMUPOL (panel A) and of ^{15}N-labeled peptide reconstituted into nonoriented membranes containing PyPol-C16 (panel B). Both samples were investigated in sapphire rotors placed into a 3.2 mm MAS probe. The ^{15}N spectra with MW ON (black; T = 112 K) and OFF are shown (gray; T = 101 K). The cooling gas causes residual spinning speeds of 5 Hz in this "pseudo-static" mode for the sample made of frozen "DNP juice" (A), and 20 Hz for the frozen membrane sample (B). The number of scans are for the spectra shown in panel A: 8 (MW ON) and 32 (MW OFF) and panel B: 256 and 18224 scans, respectively. For each panel, the spectra are scaled to the number of scans, thereby, comparison of their intensities represents the DNP scaling factor ε.

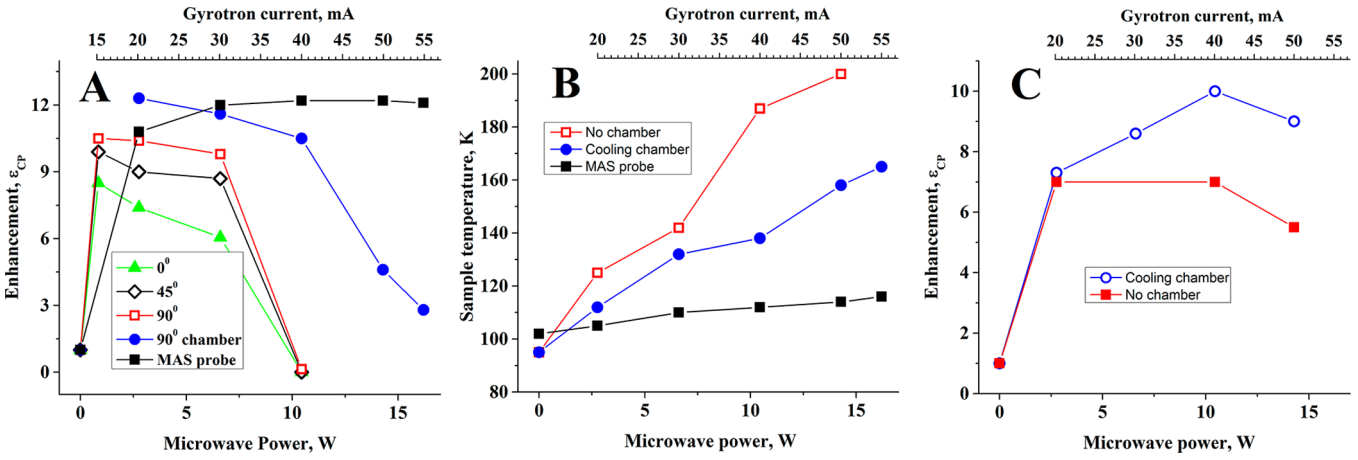

Figure 4. DNP enhancements as a function of microwave intensity for 1.5 M $^{15}NH_4Cl$ in glycerol/water ("DNP juice") in the presence of AMUPOL (panels A and B) or for ^{15}N-peptide/membrane in the presence of PyPol-C16 (panel C). The samples were placed inside sapphire rotors in the static probe (Figure 1). (A) Experimentally measured enhancement as a function of the microwave power for three different coil orientations of the static probe with and without cooling chamber and comparison with the MAS probe in its static mode. (B) Sample temperature in the static probe with and without cooling chamber. (C) DNP enhancements obtained for the membrane sample with and without cooling chamber. The microwave power and the corresponding gyrotron currents are indicated. The signal enhancements are calculated from the integrals of the resonances. Figure S2 shows the NMR line width as a function of temperature (calibration curve).

distribution obtained in the stack samples are shown in Figure 2. The mean H field is analyzed in the sample material inside the coil and is converted to units of magnetic flux density B.

In the rotor reference sample, the mean B_{1S} field is 18.2 μT/Sqrt(W) for mode 1 and 17.4 μT/Sqrt(W) for mode 2. In the stacked biomembrane samples, the variation found between mode 1 and 2 is also less than 10%, but the mean field is higher in the stack with HDPE substrate. Compared to the mean field in the glass stack, it is 15% higher for mode 1 and 34% higher for mode 2. In absolute numbers, the predicted B_{1S} field is 16−17 μT/Sqrt(W) for the glass substrate and 20−22 μT/Sqrt(W) for the HDPE substrate. It shall be noted that the absolute amount of bilayer sample is higher in the case of HDPE because the thickness of the support is 10-fold lower, such that more sample layers can be fitted into the sample stack.

The variation in mean field being less than 10% between excitation with mode 1 as opposed to mode 2 indicates that the coil is penetrable to the incident beam regardless of its polarization. Nevertheless, there is some variation in the field pattern. The presence of the stack leads to multiple reflections between the material boundaries, as well as diffraction, leading to inhomogeneous field patterns.

Performance of the DNP/Solid-State NMR Probe. In order to test RF performance of the static DNP probe shown in the Figures 1 and S3 with coil dimensions of 4 × 4 × 10 mm, the RF performance was measured with the goal to perform

DOI: 10.1021/acs.jpcb.5b07341
J. Phys. Chem. B XXXX, XXX, XXX−XXX

Lee−Goldberg decoupling and cross-polarization as typically applied (e.g., in separated local field experiments).[42] In order to obtain B_1 fields of 50 kHz at 112 K 19.1 W were applied to the ^{1}H channel and 125 W to the ^{15}N channel (measured on a glassy sample made from a solution of 1.5 M $^{15}NH_4Cl$ in glycerol/water with 10 mM AMUPOL). At room temperature, 33.2 and 235 W (solid $^{15}NH_4Cl$ powder), respectively, were required.

We then compared the static and the commercially available MAS 3.2 mm triple resonance solid-state NMR/DNP probes using two types of sample, namely "DNP juice" with AMUPOL as polarizing agent and a lipid membrane sample containing PyPol-C16 as polarizing agent (non oriented vesicles) both inside sapphire rotors. It should be noted that these rotors remain truly static in the flat-coil probe, whereas they turn slowly (5 to 20 Hz) inside the MAS probe due to the incoming cooling gas. The ^{1}H−^{15}N cross-polarization experiments of the two samples exhibited DNP enhancement factors of 12 and 14, respectively, when the microwave on and off conditions are compared to each other (Figure 3). Comparison with room-temperature spectra is difficult as on the one hand the ammonium chloride containing water/glycerol sample is in the liquid state, thus preventing cross-polarization. On the other hand. the room-temperature static cross-polarization ^{15}N spectra of the membranes (i.e., the sample from Figure 3B) exhibit distorted powder pattern line shapes ("magic angle hole", cf. ref 43) with about half the integrated signal intensity (not shown) when compared to the spectrum obtained at 100 K without microwave irradiation (LT-OFF; Figure 3B).

In the static probe, similar enhancement factors were obtained for the sample made from "DNP juice" when the integrals of the resonance were analyzed. When the microwave intensity was increased by turning the current of the gyrotron from 20 mA to 40 mA, a 17.5-fold enhancement of the peak height was transformed into a 25-fold increase. However, because at the same time the lines became narrower, the enhancement was reduced from 12.3-fold at 20 mA to 10.5-fold at 40 mA when analyzed from the integral of the resonances (Table S1, Figure 4A). When the gyrotron current is further increased, a decrease in both enhancements and line width are observed. In order to analyze these data in a more quantitative manner, the line shape was correlated to changes in the temperature using a calibration curve obtained with the same sample in the MAS probe (Figure S2). Notably, due to the microwave and RF irradiation the temperature at the sample may be higher as the one measured at the thermocouple which records the temperature of the gas outside the coil (Figure S4). Table S1a indicates the gradual increase in signal enhancement and temperature when the microwave power increases. However, when the glass melting temperature of ∼160 K is nearly reached in the sample, the enhancement suddenly drops.

Clearly an efficient cooling arrangement is essential for these experiments in order to carry away the high amount of heat induced by the microwaves. Upon an increase of microwave power by 5W, an increase in temperature of about 20 K is observed with the cooling chamber, and this effect doubles when the sample chamber was removed (Figure 4A,B). Because in this configuration the stream of cold gas is inefficient in cooling the sample, a sudden drop in DNP efficiency occurs already at 40 mA (corresponding to 10.5 W input power at the entry to the probe body). However, this "open arrangement" allowed us to optimize the relative alignment of the incoming microwave polarization and the coil, which clearly varies significantly with the relative orientation of the guide and the coil (Figure 4A), in agreement with the simulations of the field distributions within the sample predicting more shielding in mode 1 (Figure 2).

Notably, the experimentally obtained DNP enhancement varied between different orientations of the coil with respect to the incoming beam. For the 90° orientation, which corresponds to mode 1, a higher enhancement was found than for 0° orientation. This corresponds to the variation of the mean H field that was found from the electromagnetic simulations of the respective setup with the rotor sample, although the numerical results only showed a slight increase in mean field for mode 1. However, a quantitative comparison is difficult since a field distribution is obtained from the simulations, but enhancement is obtained from experiments. Furthermore, the enhancement is also a function of the temperature, which itself has been shown to change depending on the power of the beam.

DNP Enhancements with Nonoriented Membrane Samples. When nonoriented membrane samples (vesicle paste) inside a sapphire rotor (Figure 3B) were investigated with the static DNP probe, an enhancement factor of 10 was observed at 40 mA (Figure 4C, Table S2). In contrast to the ammonium chloride sample, the temperature determination through the resonance line width as demonstrated in Figure S2 is not possible. However, under these conditions a collapse of the ^{1}H line width is observed upon microwave irradiation, suggesting that the membrane-associated water undergoes a phase transition. When the ^{1}H signal of this sample was analyzed as a function of temperature, a melting point for membrane-associated water was observed at >240 K. Therefore, it is quite likely that sample heating is a reason for the lower DNP enhancement factor in the static probe (ε = 10; Figure 4C, Table S2) when compared to the pseudostatic MAS probe (ε = 12; Figure 4A). Indeed, the ^{1}H line shape suggests that even with the cooling chamber the microwave irradiation heats the sample in the static sapphire rotor to ∼250 K at 60 mA (Table S2). Furthermore, in a truly static mode, the microwaves enter the sample from one side only, whereas slow turning of the sample should allow a more even penetration of microwaves as well as a more equal exposure to the cooling gas (which also enters in a directional manner). In this context, it is noteworthy that fast MAS spinning at about 3 kHz has additional effects on the quantum transitions and results in several-fold increased enhancement factors when compared to the "pseudostatic" mode,[18,32] an effect which is also reproduced in this work where enhancements of about 35-fold and about 100-fold are observed for the membrane and the reference sample made from "DNP juice", respectively (Figure S6).

Optimizing the Preparation of Supported Lipid Bilayers for Alignment and DNP. In a next step, membranes oriented along mechanical supports were prepared. In order to test DNP efficiency and signal alignment, two different approaches were chosen. First the samples were applied onto ultrathin glass plates, a protocol that is well established at room temperature where the solid support provides well-aligned phospholipid bilayers.[37] Second, polymer films (e.g., HDPE) have been used to prepare oriented samples[20] also for magic angle oriented sample spinning (MAOSS) experiments[44] including for our very first DNP/solid-state NMR experiments on oriented membranes.[27] These materials are more flexible, and therefore, special precautions have to be taken during preparation and handling of the oriented bilayers. Here we used

DOI: 10.1021/acs.jpcb.5b07341
J. Phys. Chem. B XXXX, XXX, XXX−XXX

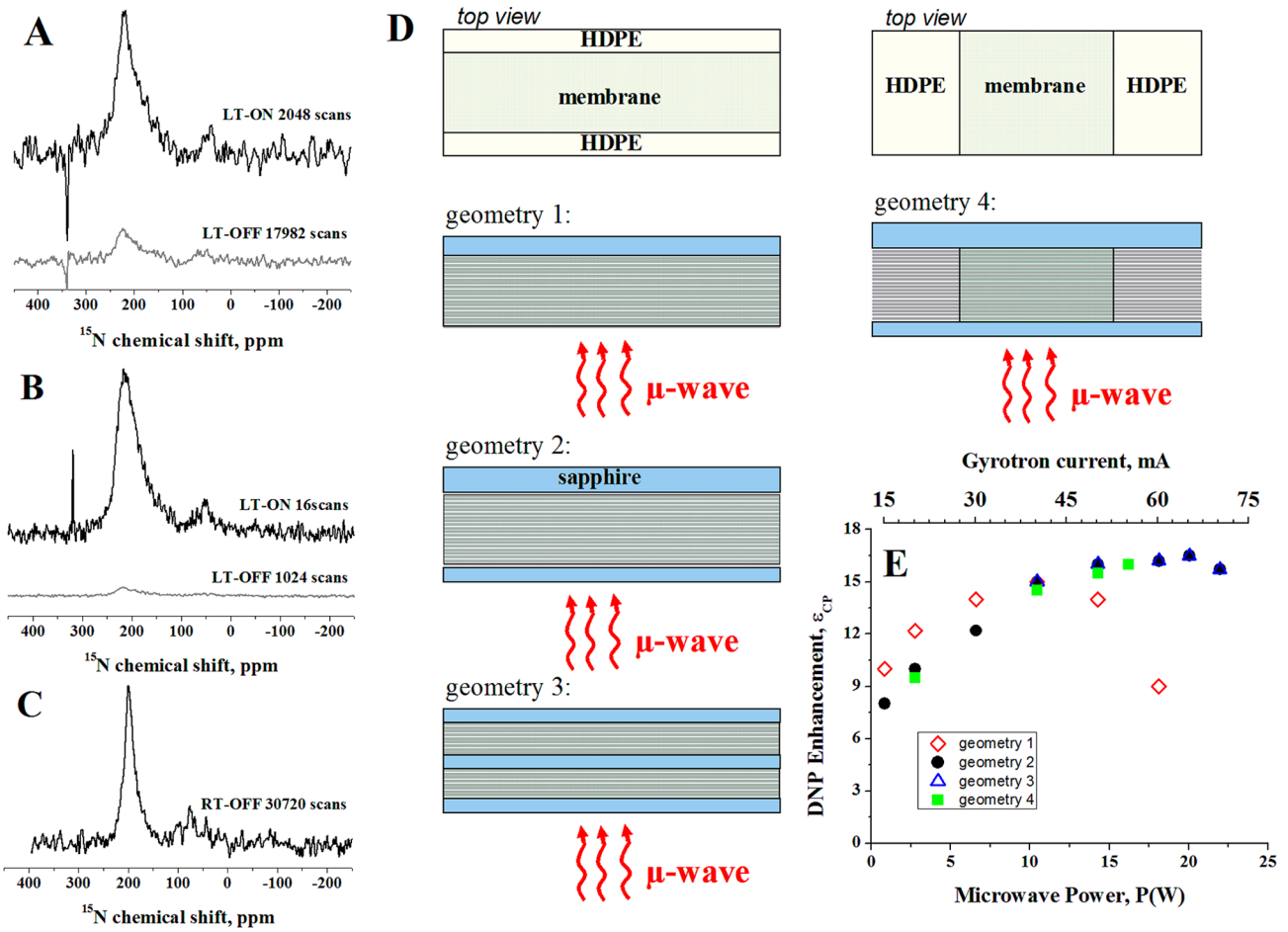

Figure 5. Proton-decoupled ^{15}N-cross-polarization spectra of [$^{15}N_5$]-hΦ19W in POPC with PyPol-C16 biradical oriented on glass plates (A; DNP enhancement 4.3-fold at 2.8 W (20 mA) microwave power) or on HDPE film (B; enhancement 16.5 at 20 W (65 mA), sample geometry 2). The ^{15}N spectra with MW ON (black) and OFF are shown (gray). Whereas the temperatures measured with the thermocouple next to the sample are around 96 K, the sample temperature under MW ON is estimated around 180 K (cf. Figure S2). (C) For comparison, the spectrum obtained at room temperature from sample B is also shown. (D) Illustration of different sample geometries obtained with the polyethylene (HDPE) films and (E) the corresponding DNP enhancements as a function of microwave power. The number of scans are for the spectra shown in panel A: 2048 (MW ON) and 17 982 (MW OFF), panel B: 16 and 1024 scans, respectively, panel C: 30 720 scans. The spectra in A and B are scaled to the number of scans and represent the DNP scaling factor ε, the spectrum in panel C is represented of similar height for comparison with panel B.

two thin sapphire plates to support the sample configuration. The experimental setup is sketched in Figure 5D.

The enhancement is considerably better when the HDPE stacks were investigated (cf. Figure 5A,B). This is probably due to the thermal insulation of the glass, which prevents the heat produced by the microwaves to be conducted efficiently to the surface of the sample where it can be cooled by the gas stream. As a consequence, at a gyrotron current of 40 mA, the ^{1}H lines of these samples collapse, suggesting that temperatures ≥240 K are reached within the sample. For related reasons, sapphire MAS rotors have been found to be better suited for DNP efficiency than those made from zirconium.[33] When the membranes on HDPE stabilized by sapphire plates were investigated, enhancements of 16.5 were obtained with a gyrotron current of 65 mA.

At room temperature, the ^{15}N solid-state NMR spectrum of the same sample encompassing five overlapping ^{15}N labels (see RT-OFF spectrum in Figure 5C) is characterized by motional narrowing, a line-width of 900 Hz, and a signal-to noise of 15.6 after 30720 scans (using a 2 s recycle delay). Thereby the spectrum is considerably narrower than the ones obtained at cryo-temperatures (2200 Hz line-width, Figures 5A,B and S7). The DNP spectrum exhibits a signal-to-noise ratio of 17.6 after only 16 scans (and was thus obtained in less than 1 min; Figure 5B). Despite the line broadening under cryo-temperature and DNP conditions, the experimental time is ∼1630 shorter, which corresponds to a 40-fold gain in sensitivity when compared to room temperature measurements.

It should be noted that the enhancements obtained here cannot directly be compared to those obtained in DNP/MAS solid-state NMR experiments for several reasons. First, the samples here are truly static samples where enhancement factors 5−10 times below those obtained under MAS conditions are observed (Figure S6), beacuse sample spinning helps in making more polarizing agents active in the sample.[18,32] Second, magic-angle spinning (or turning) probably also helps in cooling/irradiating the sample more uniformly. Third, most of the work on biradicals has aimed to optimize the conditions for glasses made of solutions where the biradicals distribute in a homogeneous manner. This is not as easy to achieve in matrix-free samples,[45] including oriented lipid bilayers where the biradicals tested so far tend to accumulate at the membrane interface.[28] Therefore, first attempts to improve the biradical distribution have been made for example by

DOI: 10.1021/acs.jpcb.5b07341
J. Phys. Chem. B XXXX, XXX, XXX−XXX

anchoring the biradicals in a more controlled manner to the lipid bilayer.[46−48] Clearly, there is a need to optimize the interactions and distribution of the polarizing agents within the sample when heterogeneous samples without a glassy matrix are investigated. Such samples require, for instance, control of the nonuniform DNP enhancement and paramagnetic-induced shifts across the various resonances. Furthermore, specifically designed polarizing agents for oriented membrane samples need to take into account the change of electron relaxation and polarization that distributes as a gradient in the sample. The Pypol-C16 was designed with these considerations in mind and shows indeed improved enhancement in membrane environments over other biradicals tested by us before.[27,28] Its synthesis and properties will be discussed in a comparative manner elsewhere.

The sapphire plates not only stabilize the HDPE stacks but they may also help in propagating the microwaves and cooling the sample.[34,35] Therefore, we tested different geometrical arrangements where we varied the number of sapphire supports as well as the localization of the oriented membranes relative to the incoming microwaves (Figures 4A and 5).

The different geometries for the sample packing are shown in Figure 5D. The sample with the membrane paste concentrated in the center of the NMR coil (geometry 4) and the sample with the membrane distributed along the full length (8 mm) of the plates (geometry 2) showed no difference in the enhancement factor suggesting that microwave irradiation is distributed equally within the membrane samples in both cases. Sample geometry 3 exhibits the same enhancement as observed with arrangements 2 and 4, which indicates that the additional dielectric interfaces do not promote microwave dissipation in the same manner as previously observed with dielectric crystalline particles of ∼0.4 mm size.[35] However, it is possible that dissipation on planar rather than irregular/curved surfaces may have different effects and/or that the presence of several HDPE layers, each 0.01 mm thick, may already result in dielectric dissipation thus that the additional sapphire plate makes only a minor difference. When the sapphire plate facing the microwave beam is absent, a sudden drop in enhancement is observed when the gyrotron currents reach 40 mA (Figure 5E). This suggests that the sapphire plates shield and/or better scatter the microwaves as well as the heat produced by this irradiation.

Finally, the NMR probe was tested for its performance on a two-dimensional separated local field spectrum where the resolution in the dipolar dimension is enhanced by phase- and frequency-switched Lee−Goldberg decoupling of the homonuclear ^{1}H interactions when at the same time cross polarized with the ^{15}N nucleus.[42] The spectrum obtained at 100 K and under DNP conditions has been obtained in less than 2 h (Figure 6), whereas it takes days under standard conditions at room temperature. This model peptide is highly dynamic, and at room temperature, a relatively sharp peak is obtained (Figure 5C), which even in two-dimensional experiments causes the five resonances to collapse in a single unresolved intensity (not shown). At the low temperature, the different conformational and orientational states of the peptide are frozen, which results in a broadened line shape (see Figure S7). Nevertheless the helical wheel can be discerned in Figure 6, allowing the analysis of the tilt angle. Whereas here the purpose is to test our probe, a new membrane-anchored biradical and a number of DNP conditions for this type of spectroscopy, optimizing the spectral resolution of the sample remained out of scope in this work.

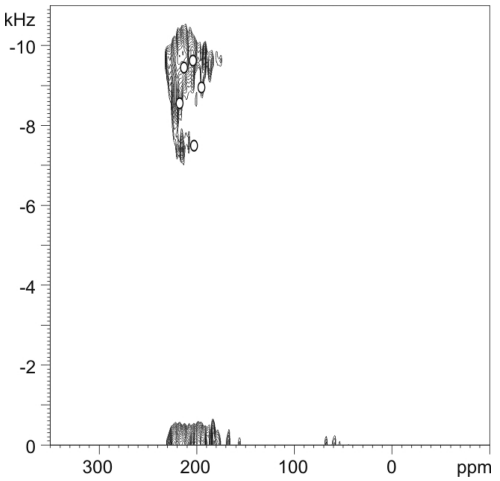

Figure 6. DNP/solid-state PISEMA spectrum of the transmembrane model peptide [^{15}N$_{5}$]-hΦ19W carrying five consecutive ^{15}N labels (3.3 mg) reconstituted into 20 mg uniaxially oriented POPC bilayers (P/L = 1/20 mol/mol) at a nominal temperature of 100 K (actual sample temperature ∼180 K) in the presence of 200 μg PyPol-C16. The DNP enhancement is 16-fold. The dots indicate a simulation of chemical shift/dipolar couplings of the five labeled sites for an ideal helix (Φ = −64°, Ψ = −41 °) at a tilt angle of 10°. The simulation was performed with Simpson,[53] in which the main tensor values were 218/79/60 ppm and 9.9 kHz for the N−H coupling.[54]

However, with the short acquisition times, the latter can be achieved by testing different temperatures (to test the effect of motional averaging), for example, by optimizing the gyrotron power against enhancement and resolution as well by varying the cooling efficiency. In addition, it has been shown that the peptide homogeneity and spectral resolution are also dependent on the membrane lipid composition.[49,50] Notably, because different conformational and topological states are trapped under the cryogenic temperatures of oriented DNP/solid-state NMR conditions, the approach probably works best for polypeptide sequences that are characterized by a rigid packing and uniform conformational features.[51,52]

In conclusion, a triple-resonance flat-coil solid-state NMR probe with microwave irradiation capacities was assembled which allows DNP/solid-state NMR experiments of static samples at temperatures of 100 K. The probe performance allows for two-dimensional separated local field experiments with high-power Lee−Goldberg decoupling and cross-polarization under simultaneous irradiation from a gyrotron microwave generator. Importantly, efficient cooling of the sample, which needed to be optimized against the microwave input proved essential for best enhancements and line shape. The geometry of supported lipid bilayers encompassing a labeled membrane polypeptide (uniaxially oriented membranes) was optimized taking into consideration membrane alignment, heat intake, handling, stability, and filling factor of the coil. Similar or even larger DNP enhancement factors were obtained using the newly developed static probe designed for oriented membrane samples relative to recently reported MAS solid-state NMR/DNP experiments on peptides in liposomes,[46−48] demonstrating that DNP/solid-state NMR can be successfully expanded to specific systems and challenging samples. By testing a new membrane-anchored biradical first two-dimensional PISEMA spectrum of a transmembrane helical peptide was obtained in less than 2 h. The shortening of acquisition times by orders of magnitude should make two- and

DOI: 10.1021/acs.jpcb.5b07341
J. Phys. Chem. B XXXX, XXX, XXX−XXX

three-dimensional solid-state NMR experiments routinely accessible also for oriented membrane samples.[55] Additional improvements will be possible with even better biradicals, different lipid compositions, and further optimized sample preparation protocols especially designed for oriented membrane systems.

■ ASSOCIATED CONTENT

Supporting Information

The Supporting Information is available free of charge on the ACS Publications website at DOI: 10.1021/acs.jpcb.5b07341.

Structure of PyPolC16, temperature calibration curve using the NH_4Cl line width, details on the probe electronic circuit and cooling chamber, engancement factors as a function of sample spinning, information on the line shapes of a transmembrane model peptide, and correlations between microwave irradiation, line shape and temperature (PDF)

■ AUTHOR INFORMATION

Corresponding Authors

*E-mail: bechinge@unistra.fr. Tel.: + 33 3 68 85 13 03. Fax: + 33 3 68 85 17 35.

*E-mail: Frank.Engelke@bruker.com. Fax: +49721516191129. Tel.: +4972151616129.

Notes

The authors declare no competing financial interest.

■ ACKNOWLEDGMENTS

We are grateful to Melanie Rosay, Werner Maas, and Alain Belguise for continuous support and discussions as well as for making available time at the DNP instrument. We also acknowledge the technical help by Delphine Hatey during peptide synthesis and preparation. The grant by the CNRS and Buker Biospin, France, to fund the Ph.D. position of H.S. has been a great encouragement to us. Furthermore, the financial contributions of the Agence Nationale de la Recherche (projects ProLipIn 10-BLAN-731, membraneDNP 12-BSV5-0012 and the LabEx Chemistry of Complex Systems 10-LABX-0026_CSC), the University of Strasbourg, the CNRS, the Région Alsace and the RTRA International Center of Frontier Research in Chemistry are gratefully acknowledged.

■ ABBREVIATIONS USED

CP	cross-polarization
DNP	dynamic nuclear polarization
EPR	electron paramagnetic resonance
HDPE	high-density polyethylene
LT	low temperature
MAS	magic angle sample spinning
NMR	nuclear magnetic resonance
P/L	peptide-to-lipid ratio
POPC	1-palmitoyl-2-oleoyl-*sn*-glycero-3-phosphocholine
PTFE	polytetrafluorethylene
RF	radio frequency
RT	room temperature

■ REFERENCES

(1) Hong, M.; de Grado, W. F. Structural Basis for Proton Conduction and Inhibition by the Influenza M2 Protein. *Protein Sci.* **2012**, *21*, 1620−33.

(2) Gustavsson, M.; Verardi, R.; Mullen, D. G.; Mote, K. R.; Traaseth, N. J.; Gopinath, T.; Veglia, G. Allosteric Regulation of Serca by Phosphorylation-Mediated Conformational Shift of Phospholamban. *Proc. Natl. Acad. Sci. U. S. A.* **2013**, *110*, 17338−17343.

(3) Baker, L. A.; Baldus, M. Characterization of Membrane Protein Function by Solid-State NMR Spectroscopy. *Curr. Opin. Struct. Biol.* **2014**, *27*, 48−55.

(4) Ong, Y. S.; Lakatos, A.; Becker-Baldus, J.; Pos, K. M.; Glaubitz, C. Detecting Substrates Bound to the Secondary Multidrug Efflux Pump EmrE by DNP-Enhanced Solid-State NMR. *J. Am. Chem. Soc.* **2013**, *135*, 15754−15762.

(5) Eddy, M. T.; Andreas, L.; Teijido, O.; Su, Y.; Clark, L.; Noskov, S. Y.; Wagner, G.; Rostovtseva, T. K.; Griffin, R. G. Magic Angle Spinning Nuclear Magnetic Resonance Characterization of Voltage-Dependent Anion Channel Gating in Two-Dimensional Lipid Crystalline Bilayers. *Biochemistry* **2015**, *54*, 994−1005.

(6) Gattin, Z.; Schneider, R.; Laukat, Y.; Giller, K.; Maier, E.; Zweckstetter, M.; Griesinger, C.; Benz, R.; Becker, S.; Lange, A. Solid-State NMR, Electrophysiology and Molecular Dynamics Characterization of Human VDAC 2. *J. Biomol. NMR* **2015**, *61*, 311−320.

(7) Linke, D.; Shahid, S.; Habeck, M.; Bardiaux, B.; van Rossum, B. Membrane-Protein Structure Determination by Solid-State NMR Spectroscopy of Microcrystals: The Autotransport Domain of Yersinia Yada. *FASEB J.* **2013**, *27*, 590.1.

(8) Das, N.; Dai, J.; Hung, I.; Rajagopalan, M. R.; Zhou, H. X.; Cross, T. A. Structure of Crga, a Cell Division Structural and Regulatory Protein from Mycobacterium Tuberculosis, in Lipid Bilayers. *Proc. Natl. Acad. Sci. U. S. A.* **2015**, *112*, E119−26.

(9) Bechinger, B.; Sizun, C. Alignment and Structural Analysis of Membrane Polypeptides by 15N and 31P Solid-State NMR Spectroscopy. *Concepts Magn. Reson.* **2003**, *18A*, 130−145.

(10) Cross, T. A. Solid-State Nuclear Magnetic Resonance Characterization of Gramicidin Channel Structure. *Methods Enzymol.* **1997**, *289*, 672−696.

(11) Michalek, M.; Salnikov, E.; Werten, S.; Bechinger, B. Structure and Topology of the Huntingtin 1−17 Membrane Anchor by a Combined Solution and Solid-State NMR Approach. *Biophys. J.* **2013**, *105*, 699−710.

(12) Aisenbrey, C.; Bechinger, B. Tilt and Rotational Pitch Angles of Membrane-Inserted Polypeptides from Combined 15N and 2H Solid-State NMR Spectroscopy. *Biochemistry* **2004**, *43*, 10502−10512.

(13) Yamamoto, K.; Dürr, U. H. N.; Xu, J.; Im, S. C.; Waskell, L.; Ramamoorthy, A. Dynamic Interaction Between Membrane-Bound Full-Length Cytochrome P450 and Cytochrome B5 Observed by Solid-State NMR Spectroscopy. *Sci. Rep.* **2013**, *3*, 2538.

(14) Perrone, B.; Miles, A. J.; Salnikov, E. S.; Wallace, B.; Bechinger, B. Lipid- Interactions of the LAH4, a Peptide with Antimicrobial and Nucleic Transfection Activities. *Eur. Biophys. J.* **2014**, *43*, 499−507.

(15) Aisenbrey, C.; Sudheendra, U. S.; Ridley, H.; Bertani, P.; Marquette, A.; Nedelkina, S.; Lakey, J. H.; Bechinger, B. Helix Orientations in Membrane-Associated Bcl-X L Determined by 15N Solid-State NMR Spectroscopy. *Eur. Biophys. J.* **2007**, *37*, 71−80.

(16) Can, T. V.; Caporini, M. A.; Mentink-Vigier, F.; Corzilius, B.; Walish, J. J.; Rosay, M.; Maas, W. E.; Baldus, M.; Vega, S.; Swager, T. M.; et al. Overhauser Effects in Insulating Solids. *J. Chem. Phys.* **2014**, *141*, 064202.

(17) Ni, Q. Z.; Daviso, E.; Can, T. V.; Markhasin, E.; Jawla, S. K.; Swager, T. M.; Temkin, R. J.; Herzfeld, J.; Griffin, R. G. High Frequency Dynamic Nuclear Polarization. *Acc. Chem. Res.* **2013**, *46*, 1933−1941.

(18) Rosay, M.; Tometich, L.; Pawsey, S.; Bader, R.; Schauwecker, R.; Blank, M.; Borchard, P. M.; Cauffman, S. R.; Felch, K. L.; Weber, R. T.; et al. Solid-State Dynamic Nuclear Polarization at 263 Ghz: Spectrometer Design and Experimental Results. *Phys. Chem. Chem. Phys.* **2010**, *12*, 5850−60.

(19) Aisenbrey, C.; Michalek, M.; Salnikov, E. S.; Bechinger, B. Solid-State NMR Approaches to Study Protein Structure and Protein-Lipid Interactions. In *Lipid-Protein Interactions: Methods and Protocols*; Kleinschmidt, J. H., Ed.; Springer: New York, 2013; pp 357−387.

DOI: 10.1021/acs.jpcb.5b07341
J. Phys. Chem. B XXXX, XXX, XXX−XXX

(20) Auge, S.; Mazarguil, H.; Tropis, M.; Milon, A. Preparation of Oriented Lipid Bilayer on Ultrathin Polymers for Solid-State NMR Analyses of Peptide-Membrane Interactions. *J. Magn. Reson.* **1997**, *124*, 455−458.
(21) Prosser, R. S.; Hunt, S. A.; Vold, R. R. Improving Sensitivity in Mechanically Oriented Phospholipid Bilayers Ursing Ultrathin Glass Plates - a Deuterium Solid-State NMR Study. *J. Magn. Reson., Ser. B* **1995**, *109*, 109−111.
(22) Loudet, C.; Diller, A.; Grelard, A.; Oda, R.; Dufourc, E. J. Biphenyl Phosphatidylcholine: A Promoter of Liposome Deformation and Bicelle Collective Orientation by Magnetic Fields. *Prog. Lipid Res.* **2010**, *49*, 289−97.
(23) Prosser, R. S.; Hwang, J. S.; Vold, R. R. Magnetically Aligned Phospholipid Bilayers with Positive Ordering: A New Model Membrane System. *Biophys. J.* **1998**, *74*, 2405−2418.
(24) Thurber, K. R.; Yau, W. M.; Tycko, R. Low-Temperature Dynamic Nuclear Polarization at 9.4 T with a 30 MW Microwave Source. *J. Magn. Reson.* **2010**, *204*, 303−313.
(25) Akbey, U.; Linden, A. H.; Oschkinat, H. High-Temperature Dynamic Nuclear Polarization Enhanced Magic-Angle-Spinning NMR. *Appl. Magn. Reson.* **2012**, *43*, 81−90.
(26) Jakdetchai, O.; Denysenkov, V.; Becker-Baldus, J.; Dutagaci, B.; Prisner, T. F.; Glaubitz, C. Dynamic Nuclear Polarization-Enhanced NMR on Aligned Lipid Bilayers at Ambient Temperature. *J. Am. Chem. Soc.* **2014**, *136*, 15533−15536.
(27) Salnikov, E.; Rosay, M.; Pawsey, S.; Ouari, O.; Tordo, P.; Bechinger, B. Solid-State NMR Spectroscopy of Oriented Membrane Polypeptides at 100 K with Signal Enhancement by Dynamic Nuclear Polarization. *J. Am. Chem. Soc.* **2010**, *132*, 5940−1.
(28) Salnikov, E. S.; Ouari, O.; Koers, E.; Sarrouj, H.; Franks, T.; Rosay, M.; Pawsey, S.; Reiter, C.; Bandara, P.; Oschkinat, H.; et al. Developing DNP/Solid-State NMR Spectroscopy of Oriented Membranes. *Appl. Magn. Reson.* **2012**, *43*, 91−106.
(29) Bechinger, B.; Opella, S. J. Flat-Coil Probe for NMR Spectroscopy of Oriented Membrane Samples. *J. Magn. Reson.* **1991**, *95*, 585−588.
(30) Thurber, K. R.; Tycko, R. Perturbation of Nuclear Spin Polarizations in Solid State NMR of Nitroxide-Doped Samples by Magic-Angle Spinning without Microwaves. *J. Chem. Phys.* **2014**, *140*, 184201.
(31) Thurber, K. R.; Tycko, R. Theory for Cross Effect Dynamic Nuclear Polarization under Magic-Angle Spinning in Solid State Nuclear Magnetic Resonance: The Importance of Level Crossings. *J. Chem. Phys.* **2012**, *137*, 084508.
(32) Mentink-Vigier, F.; Akbey, U.; Hovav, Y.; Vega, S.; Oschkinat, H.; Feintuch, A. Fast Passage Dynamic Nuclear Polarization on Rotating Solids. *J. Magn. Reson.* **2012**, *224*, 13−21.
(33) Lide, D. R. E. *Properties of Solids*; CRC Press: Boca Raton, FL, 2005.
(34) Nanni, E. A.; Barnes, A. B.; Matsuki, Y.; Woskov, P. P.; Corzilius, B.; Griffin, R. G.; Temkin, R. J. Microwave Field Distribution in a Magic Angle Spinning Dynamic Nuclear Polarization NMR Probe. *J. Magn. Reson.* **2011**, *210*, 16−23.
(35) Kubicki, D. J.; Rossini, A. J.; Purea, A.; Zagdoun, A.; Ouari, O.; Tordo, P.; Engelke, F.; Lesage, A.; Emsley, L. Amplifying Dynamic Nuclear Polarization of Frozen Solutions by Incorporating Dielectric Particles. *J. Am. Chem. Soc.* **2014**, *136*, 15711−15718.
(36) Sauvee, C.; Rosay, M.; Casano, G.; Aussenac, F.; Weber, R. T.; Ouari, O.; Tordo, P. Highly Efficient, Water-Soluble Polarizing Agents for Dynamic Nuclear Polarization at High Frequency. *Angew. Chem., Int. Ed.* **2013**, *52*, 10858−10861.
(37) Aisenbrey, C.; Bertani, P.; Bechinger, B. Solid-State NMR Investigations of Membrane-Associated Antimicrobial Peptides. In *Antimicrobial Peptides*; Guiliani, A., Rinaldi, A. C., Eds. Humana Press, Springer: New York, 2010; pp 209−233.
(38) Hediger, S.; Meier, B. H.; Ernst, R. R. Adiabatic Passage Hartmann-Hahn Cross Polarization in NMR under Magic Angle Sample Spinning. *Chem. Phys. Lett.* **1995**, *240*, 449−456.
(39) Bertani, P.; Raya, J.; Bechinger, B. 15N Chemical Shift Referencing in Solid State NMR. *Solid State Nucl. Magn. Reson.* **2014**, *61*−*62*, 15−18.
(40) Salnikov, E.; Aisenbrey, C.; Raya, J.; Bechinger, B. Investigations of the Structure,Topology and Dynamics of Membrane-Associated Polypeptides by Solid-State NMR Spectroscopy. In *New Developments in NMR: Advances in Biological Solid-State NMR, Proteins and Membrane-Active Peptides*; Separovic, F., Naito, A., Eds. Royal Society of Chemistry: London, 2014; pp 214−234.
(41) Lamb, J. W. Miscellaneous Data on Materials for Millimetre and Submillimetre Optics. *Int. J. Infrared Millimeter Waves* **1996**, *17*, 1997−2034.
(42) Ramamoorthy, A.; Wei, Y.; Lee, D. Pisema Solid-State NMR Spectroscopy. *Annu. Rep. NMR Spectrosc.* **2004**, *52*, 1−52.
(43) Raya, J.; Perrone, B.; Bechinger, B.; Hirschinger, J. Chemical Shift Powder Spectra Obtained by Using Rotor-Directed Exchange of Orientations Cross-Polarization (RODEO-CP). *Chem. Phys. Lett.* **2011**, *508*, 155−164.
(44) Sizun, C.; Bechinger, B. Bilayer Samples for Fast or Slow Magic Angle Oriented Sample Spinning Solid-State NMR Spectroscopy. *J. Am. Chem. Soc.* **2002**, *124*, 1146−1147.
(45) Takahashi, H.; Lee, D.; Dubois, L.; Bardet, M.; Hediger, S.; De Paepe, G. Rapid Natural-Abundance 2D C-13-C-13 Correlation Spectroscopy Using Dynamic Nuclear Polarization Enhanced Solid-State NMR and Matrix-Free Sample Preparation. *Angew. Chem., Int. Ed.* **2012**, *51*, 11766−11769.
(46) Mao, J. F.; Akhmetzyanov, D.; Ouari, O.; Denysenkov, V.; Corzilius, B.; Plackmeyer, J.; Tordo, P.; Prisner, T. F.; Glaubitz, C. Host-Guest Complexes as Water-Soluble High-Performance DNP Polarizing Agents. *J. Am. Chem. Soc.* **2013**, *135*, 19275−19281.
(47) Smith, A. N.; Caporini, M. A.; Fanucci, G. E.; Long, J. R. A Method for Dynamic Nuclear Polarization Enhancement of Membrane Proteins. *Angew. Chem., Int. Ed.* **2015**, *54*, 1542−1546.
(48) Fernandez-de-Alba, C.; Takahashi, H.; Richard, A.; Chenavier, Y.; Dubois, L.; Maurel, V.; Lee, D.; Hediger, S.; De Paepe, G. Matrix-Free DNP-Enhanced NMR Spectroscopy of Liposomes Using a Lipid-Anchored Biradical. *Chem. - Eur. J.* **2015**, *21*, 4512−7.
(49) Lee, D. K.; Kwon, B. S.; Ramamoorthy, A. Freezing Point Depression of Water in Phospholipid Membranes: A Solid-State NMR Study. *Langmuir* **2008**, *24*, 13598−13604.
(50) Salnikov, E. S.; De Zotti, M.; Formaggio, F.; Li, X.; Toniolo, C.; O'Neil, J. D.; Raap, J.; Dzuba, S. A.; Bechinger, B. Alamethicin Topology in Phospholipid Membranes by Oriented Solid-State NMR and EPR Spectroscopies: A Comparison. *J. Phys. Chem. B* **2009**, *113*, 3034−3042.
(51) Kamihira, M.; Vosegaard, T.; Mason, A. J.; Straus, S. K.; Nielsen, N. C.; Watts, A. Structural and Orientational Constraints of Bacteriorhodopsin in Purple Membranes Determined by Oriented-Sample Solid-State NMR Spectroscopy. *J. Struct. Biol.* **2005**, *149*, 7−16.
(52) Vogt, T. C. B.; Schinzel, S.; Bechinger, B. Biosynthesis of Biochemically Labelled Gramicidins and Tyrocidins by Bacillus Brevis. *J. Biomol. NMR* **2003**, *26*, 1−11.
(53) Bak, M.; Rasmussen, J. T.; Nielsen, N. C. Simpson: A General Simulation Program for Solid-State NMR Spectroscopy. *J. Magn. Reson.* **2000**, *147*, 296−330.
(54) Salnikov, E.; Bertani, P.; Raap, J.; Bechinger, B. Analysis of the Amide (15)N Chemical Shift Tensor of the C(Alpha) Tetrasubstituted Constituent of Membrane-Active Peptaibols, the Alpha-Amino-isobutyric Acid Residue, Compared to Those of Di- and Tri-Substituted Proteinogenic Amino Acid Residues. *J. Biomol. NMR* **2009**, *45*, 373−87.
(55) Gopinath, T.; Mote, K. R.; Veglia, G. Simultaneous Acquisition of 2d and 3d Solid-State NMR Experiments for Sequential Assignment of Oriented Membrane Protein Samples. *J. Biomol. NMR* **2015**, *62*, 53.

DOI: 10.1021/acs.jpcb.5b07341
J. Phys. Chem. B XXXX, XXX, XXX−XXX